Journal of the Serbian Chemical Society
JSCS@tmf.bg.ac.rs • www.shd.org.rs/JSCS

J. Serb. Chem. Soc. 74 (8–9) 965–975 (2009)
JSCS–3891

UDC 546.923'962+544.478:66.087.3
Original scientific paper

Activity of carbon supported Pt_3Ru_2 nanocatalyst in CO oxidation

KSENIJA DJ. POPOVIĆ[1]*#, JELENA D. LOVIĆ[1#], AMALIJA V. TRIPKOVIĆ[1#] and PIOTR K. OLSZEWSKI[2]

[1]*ICTM – Institute of Electrochemistry, University of Belgrade, Njegoševa 12, P.O. Box 473, 11000 Belgrade, Serbia and* [2]*Institute of Catalysis and Surface Chemistry, Polish Academy of Sciences, Krakow, Niezapominajek 8, 30-239, Poland*

(Received 23 February, revised 24 April 2009)

Abstract: The electrocatalytic activity of Pt_3Ru_2/C nanocatalyst toward the electro-oxidation of bulk CO was examined in acid and alkaline solution at ambient temperature using the thin-film, rotating disk electrode (RDE) method. The catalyst was characterized by XRD analysis. The XRD pattern revealed that the Pt_3Ru_2/C catalyst consisted of two structures, *i.e.*, Pt–Ru-fcc and Ru-hcp (a solid solution of Ru in Pt and a small amount of Ru or a solid solution of Pt in Ru). Electrocatalytic activities were measured by applying potentiodynamic and steady state techniques. The oxidation of CO on the Pt_3Ru_2/C catalyst was influenced by pH and anions from the supporting electrolytes. The Pt_3Ru_2/C was more active in alkaline than in acid solution, as well as in perchloric than in sulfuric acid. Comparison of CO oxidation on Pt_3Ru_2/C and Pt/C revealed that the Pt_3Ru_2/C was more active than Pt/C in acid solution, while both catalysts had a similar activity in alkaline solution.

Keywords: CO oxidation; Pt_3Ru_2/C nanocatalyst; XRD; pH effect; anion effect.

INTRODUCTION

The major interest for the electro-oxidation of CO on a Pt_3Ru_2/C catalyst originated from previous studies of the electrocatalytic activity on PtRu-supported nanocatalysts in the electro-oxidation of methanol and formic acid.[1–6] The electro-oxidations of methanol and formic acid, anodic reactions in fuel cells, belong to typical auto-inhibiting reactions producing strongly bound intermediates (predominantly CO-type species), well known as catalytic poisons.[7] The oxidative removal of adsorbed CO by adsorbed oxygen containing species plays a dominant role in determining the catalyst activity in these reactions.

* Corresponding author. E-mail: ksenija@tmf.bg.ac.rs
# Serbian Chemical Society member.
doi: 10.2298/JSC0909965P

It is believed that the electro-oxidation of CO_{ad} on an electrode surface in an electrolyte occurs analogously to the oxidative removal of CO on a Pt surface in the gas phase, which proceeds *via* the Langmuir–Hinshelwood mechanism, *i.e.*, by reaction of chemisorbed CO with chemisorbed oxygen.[8,9]

The superior activity of PtRu among other catalytic materials has been explained by a bifunctional mechanism in which the oxidation of adsorbed CO is facilitated by the presence of OH_{ad} species formed by the electrochemical dissociation of water on oxophilic surface atoms, such as Ru, at lower anodic overpotentials compared with pure Pt.[10,11] Consequently, the Ru sites act as collectors for OH_{ad} species, which then catalyze the oxidation of CO molecules preferentially bonded to neighboring Pt atoms. Additionally, the so-called ligand or electronic effect, in which the Ru alters the electronic properties of the Pt, might also be considered.[8,12]

In this study, the electrocatalytic activity of a Pt_3Ru_2/C catalyst in the electro-oxidation of bulk CO was examined in acid and alkaline solution at ambient temperature in order to study the effects of pH and anions of the electrolytes. Activity of the Pt_3Ru_2/C was compared with activity of a Pt/C catalyst. A quasi--bifunctional mechanism for CO bulk oxidation on both catalysts in acid and alkaline solution is proposed.

EXPERIMENTAL

Electrode preparation

High area carbon supported platinum–ruthenium (Pt_3Ru_2/C) and platinum (Pt/C) nanocatalysts with 33.5 wt % alloy and 47.5 wt % Pt (Tanaka Precious Metal Group, Tokyo, Japan) were applied to a glassy carbon substrate in the form of a thin-film.[13] A suspension of Pt_3Ru_2/C or Pt/C in water was prepared in an ultrasonic bath and a drop of the suspension was placed onto the substrate, resulting in the constant loading of 15 μg_{Alloy} cm^{-2} or 20 μg_{Pt} cm^{-2}, respectively. After drying in a stream of high-purity nitrogen at room temperature, the deposited catalyst layer was covered with 20 µl of a diluted aqueous Nafion® solution (thickness *ca*. 0.1 µm) and left to dry completely.

Mass transfer resistance through the Nafion® film covering the Pt_3Ru_2/C layer was determined by recording the diffusion limiting currents of hydrogen oxidation on the rotating disk electrode. Since a Levich–Koutecky plot with an intercept close to zero was obtained, it was concluded that the mass transfer resistance through the Nafion® film was negligible.[1]

Electrode characterization

The carbon supported Pt and Pt_3Ru_2 catalysts were characterized by X-ray powder diffraction analysis using a Siemens D5005 (Bruker-AXS, Germany) diffractometer system, equipped with a CuKα source operating at 40 mA and 40 kV and graphite monochromator. The XRD patterns were obtained in the 2θ range 10–100°, with 0.01°/s steps. The quantitative analysis of the phase content and crystallite size calculations were performed by multiphase Rietveld refinement using Topas software and the Fundamental Parameters approach for the modeling of the peak shape.

Electrochemical measurements

All electrochemical measurements were conducted in a thermostated three-compartment electrochemical cell at ambient temperature. The reference electrode was a standard calomel electrode (SCE) separated from the working electrode compartment to avoid chloride contamination. The potentials in this study were referred to the reversible hydrogen electrode (RHE).

The thin film rotating disk method was used for the determination of the catalytic activity. The rotation rate was 2000 rpm. All solutions were prepared with high purity water ("Millipore", 18 MΩ cm resistivity) and p.a. (H_2SO_4 and NaOH) or ultra high purity ($HClO_4$) grade chemicals (Merck). The $HClO_4$ was without any trace of Cl ions. The prepared electrodes were immersed in nitrogen purged perchloric or sulfuric acid or sodium hydroxide solution to record the basic voltammograms.

Carbon monoxide adsorption was performed in CO saturated solution holding the electrodes at 0.05 V for 3 min. The supporting electrolytes were saturated with CO by bubbling high purity CO through the solution for 30 min. The cyclic voltammograms were recorded using a sweep rate of 50 or 1 mV s^{-1}.

RESULTS AND DISCUSSION

Characterization of the catalysts

The XRD patterns of the carbon-supported Pt and Pt_3Ru_2 catalysts are shown in Fig. 1. The four characteristic peaks of the face-centered cubic (fcc) crystalline structure of Pt/C are seen: (111), (200), (220) and (311).

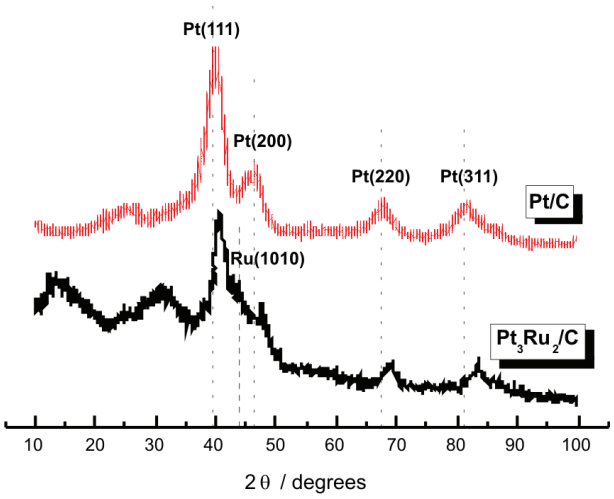

Fig. 1. XRD Patterns of Pt_3Ru_2/C and Pt/C catalysts. The vertical lines represent the positions of the peaks of pure Pt and pure Ru.

Two phases were identified in the diffraction pattern of the Pt_3Ru_2/C catalyst: a solid solution of ruthenium in platinum (fcc) and a phase associated with a weak peak at 43.8° assigned to the strongest Ru(1010) peak in the hexagonal phase of ruthenium (hcp). The first two broad peaks at 14.0 and 30.9° were assigned to the carbon support material. The Pt–Ru-fcc reflections in the Pt_3Ru_2/C

pattern were systematically shifted towards higher angles in relation to the pure platinum peaks in the pattern of the Pt/C catalyst, due to the incorporation of smaller ruthenium atoms into platinum crystal lattice.[14] The lattice parameter for the Pt_3Ru_2/C catalyst (3.859(8) Å) was smaller than that of Pt/C (3.916(6) Å), due to a lattice contraction caused by the incorporation of Ru into the *fcc* structure of platinum after alloying. On the other hand, the presence of the 43.8° peak, attributed to the Ru-hcp phase, indicates that this incorporation was only partial. It was assumed in the calculations that the second phase is Ru-hcp.

The two structures, *i.e.*, Pt–Ru-fcc and Ru-hcp, were refined using the Rietveld method. The presence of the carbon support was not taken into account. The crystallite size determined using the Scherrer method, based on the broadening of the (220) peak, was 3.1 nm for the Pt and 4.5 nm for Pt–Ru-fcc phase, respecttively. Similar crystallite sizes for both catalysts were calculated from the charge under the CO stripping peaks.

The carbon supported Pt_3Ru_2 nanocatalyst was examined in acid and alkaline solution at ambient temperature. The obtained voltammetric profiles (Fig. 2) can be divided into two regions: hydrogen desorption/adsorption between 0.05 V and 0.30 V and adsorption/desorption of reversible and irreversible oxygen-containing species, such as RuOH, Ru_2O, RuO_xH_2O, *etc.*,[15,16] at more positive potentials. The continuous and fast transition from the reversible to irreversible state of the oxides resulted in a broad capacitive feature in the profile of the PtRu alloy. The anodic limit was set to 0.80 V to prevent any Ru dissolution.[17]

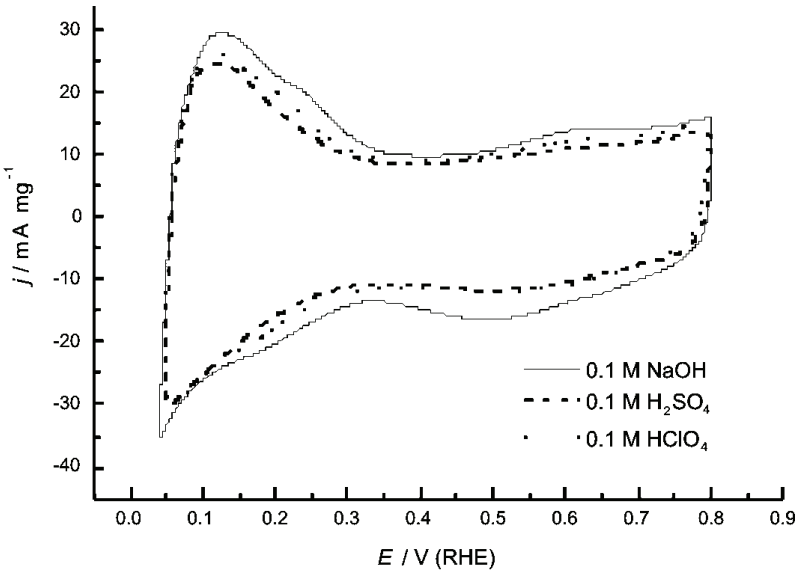

Fig. 2. Cyclic voltammograms of a high surface area Pt_3Ru_2 catalyst in alkaline and two different acid solutions. ω = 2000 rpm; ν = 50 mV s^{-1}; T = 295 K.

Potentiodynamic measurements

The electrocatalytic activities of Pt_3Ru_2/C catalyst in the bulk oxidation of CO were examined in acid and alkaline electrolytes in order to establish the effects of anions and the pH of the solution.

Effect of anions. The role of anions in the supporting electrolyte ($HClO_4$ and H_2SO_4) on the kinetics of CO oxidation can be seen from the corresponding voltammograms given in Fig. 3. To avoid any influence of chlorides present in *p.a.* perchloric acid, ultra high pure $HClO_4$ (without any traces of Cl^-) was employed. Evidently, bisulfates influence the beginning of the reaction, slightly shifting the onset potential towards higher values relative to $HClO_4$. This phenomenon was also observed in methanol oxidation.[5,18] Bisulfates decrease the activity of Pt_3Ru_2/C in the oxidation of CO due to their competition with OH and CO for adsorption on Pt sites freed from CO_{ad}.

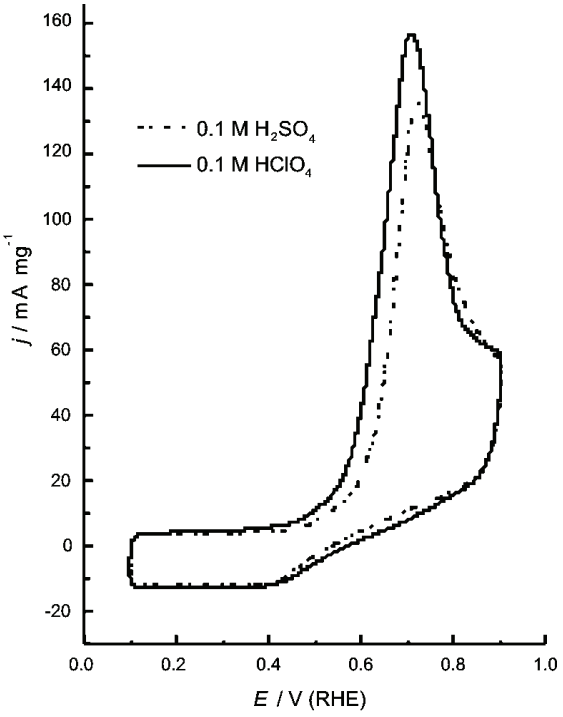

Fig. 3. Cyclic voltammograms for the oxidation of bulk CO on a Pt_3Ru_2/C electrode in 0.10 M H_2SO_4 and 0.10 M $HClO_4$ solutions. ω = 2000 rpm; ν = 50 mV s^{-1}; T = 295 K.

Effect of pH. The cyclic voltammograms for CO oxidation in acid ($HClO_4$) and alkaline (NaOH) solutions are shown in Fig. 4. The reaction commences at a $\approx$ 0.1 V more negative potential in NaOH than in $HClO_4$ media, suggesting clearly that the alkaline solution promotes CO oxidation. This is evidence that Pt can adsorb OH species in alkaline solution at significantly lower potentials than in acid solutions.

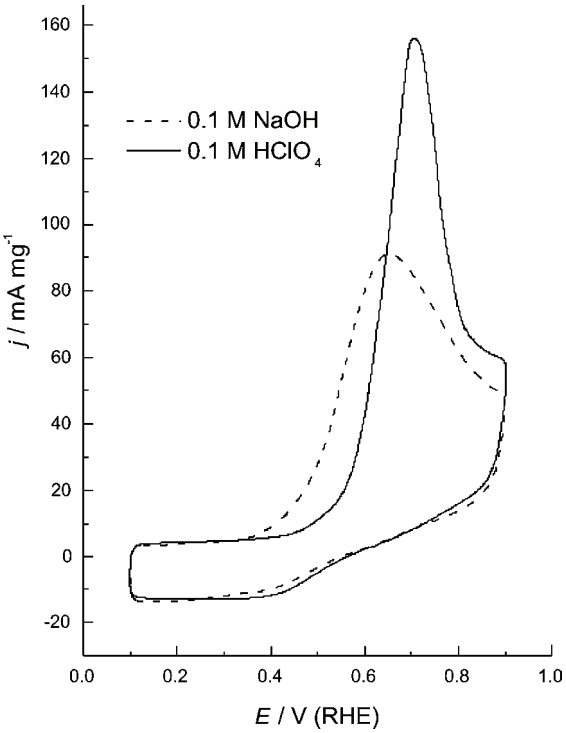

Fig. 4. Cyclic voltammograms for CO bulk oxidation on a Pt_3Ru_2/C electrode in 0.10 M NaOH and 0.10 M $HClO_4$ solutions. ω = 2000 rpm; ν = 50 mV s^{-1}; T = 295 K.

Quasi-steady state measurements

The quasi-steady state curves for CO oxidation recorded at a slow sweep of 1 mV s^{-1} in acid and alkaline solutions are presented in Fig. 5. The general trends observed in the potentiodynamic experiments were also observed in the quasi--steady state measurements. The oxidation of CO was significantly enhanced in alkaline relative to acid media. The onset of the reaction was shifted by ≈ 0.10 V towards less positive potentials and the current densities were higher by more than one order of magnitude. The faster kinetics achieved in perchloric acid than in sulfuric acid by a factor of ≈ 2 indicates inhibition of CO oxidation caused by bisulfate adsorption.

The slopes of the Tafel lines for CO bulk oxidation on the Pt_3Ru_2/C catalyst were ≈ 120 mV dec^{-1}. This fact implies the same limiting step in CO oxidation according to a Langmuir–Hinshelwood type reaction[8] in all the studied media.

Comparison of CO oxidation on Pt_3Ru_2/C and on Pt/C catalysts

The oxidation of CO on Pt_3Ru_2/C and Pt/C catalysts in acid and alkaline solutions are shown in Fig. 6a and 6b, respectively.

CO oxidation on a Pt/C catalyst in H_2SO_4 solution is represented by a sharp, symmetric peak centered at approximately 0.90 V and by a so-called pre-wave, in

the potential region 0.40 V < E < 0.80 V. The pre-wave, appearing in the pre-ignition region of CO oxidation, is related to the oxidation of CO on defect sites on the facets.[19] It is also a characteristic of CO oxidation on low-index Pt single crystal surfaces, where it was correlated with the presence of nano-islands on the terraces.[20]

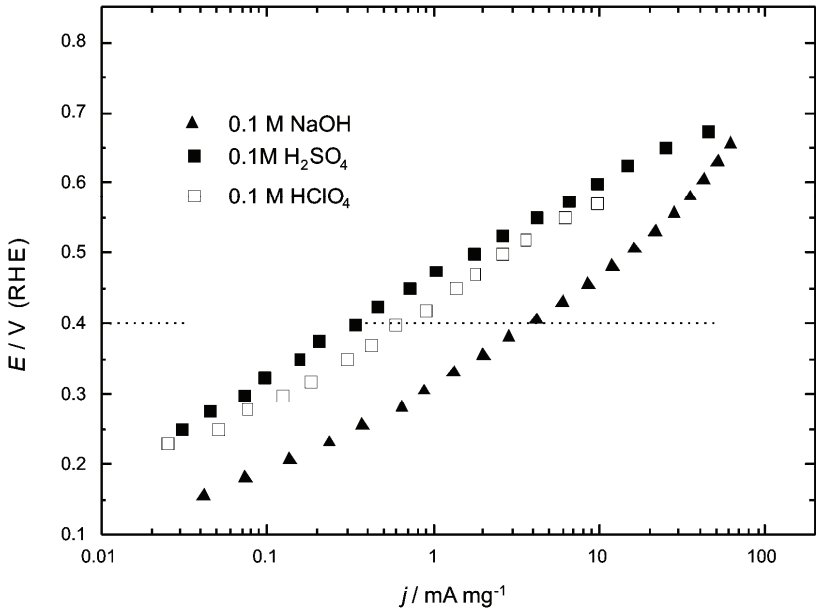

Fig. 5. Mass-specificquasi-steady state current densities for CO oxidation on a Pt_3Ru_2/C nanocatalyst in three different solutions. ω = 2000 rpm; ν = 1 mV s^{-1}; T = 295 K.

Interestingly, CO oxidation on Pt_3Ru_2/C occurs in the potential region assigned as the preignition region on Pt/C, but the reaction rate is significantly enhanced compared to Pt/C. This is important datum suggesting that both metals, Ru and Pt, are able to adsorb OH species at ≈ 0.40 V. However, the reaction rate on Pt_3Ru_2/C is significantly increased, implying that the coverage by OH_{ad} species is larger on Ru than on Pt sites. It should be noted that under these experimental conditions, a high and constant coverage by CO_{ad} was achieved on both electrodes at the onset potential.[21,22] Anions (bisulfates) did not affect CO adsorption at 0.05 V, which is in accordance with the results reported in the literature.[23]

In alkaline solution, CO oxidation commenced at ≈ 0.3 V on both catalysts. Additionally, both catalysts exhibit similar activity at potentials of technical interest (E < 0.6 V). This is clear evidence that in alkaline solution not only Ru but also Pt becomes able to form OH_{ad} species at low potentials.

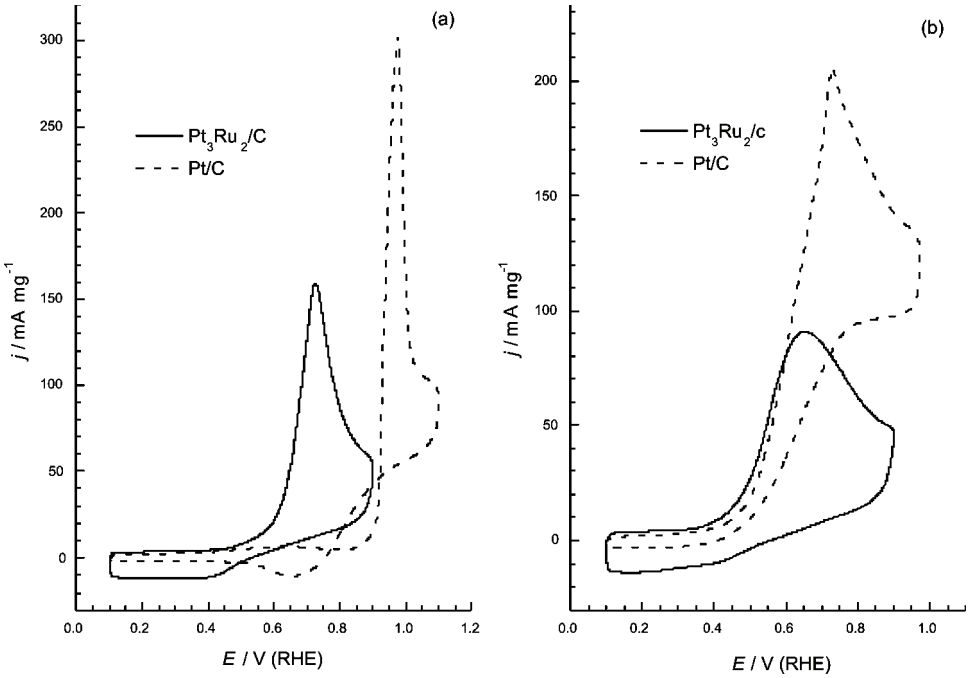

Fig. 6. Cyclic voltammograms for the oxidation of bulk CO on Pt_3Ru_2/C and Pt/C catalysts in (a) 0.10 M H_2SO_4 and (b) in 0.10 M NaOH solutions. ω = 2000 rpm; ν = 50 mV s^{-1}; T = 295 K.

CO electro-oxidation mechanism

The oxidation of CO on Pt and PtRu alloy surfaces is consistent with a Langmuir–Hinshelwood reaction mechanism between adsorbed CO and oxygen--containing species, OH_{ad}. The formation of CO_{ad} occurs with equal facility on Ru and Pt sites, while the nucleation of OH_{ad} at low electrode potentials is specific to Ru surface atoms in acid solution.

According to the bifunctional mechanism,[10] the electro-oxidation of CO molecules on a Pt_3Ru_2/C surface could be presented in two major steps. The first step is nucleation and growth of oxygen-containing species on the Ru sites at significantly more negative potentials compared to Pt sites:

$$Ru + H_2O \rightarrow Ru–OH_{ad} + H^+ + e^- \quad (1)$$

which can then initiate further electro-oxidation of CO molecules adsorbed on either Pt or Ru neighboring sites. This step occurs at surface sites referred to as “active sites”. On bulk Pt electrodes, the splitting of water probably occurs on particular sites, such as crystalline defects.[24] On carbon-supported Pt nanoparticles, it was proposed that these sites are defects of cubo-octahedral structure.[25]

The second step is the reaction between the adsorbed oxygenated species and CO_{ad}, yielding CO_2 as the final product:

$$CO_{ad} + OH_{ad} \rightarrow CO_2 + H^+ + e^- \quad (2)$$

In this study, the onset potential for the oxidation of CO_{ad} at a Pt_3Ru_2/C catalyst was shifted towards negative potentials in acid solution compared to Pt, which is characteristic of a bimetal Pt/Ru structure. As the coverage with CO_{ad} was high, the reaction was limited by water splitting (Eq. (1)), which may explain the higher activity of Pt_3Ru_2/C than Pt/C in acid solution.

In alkaline solution, the adsorption of oxygen-containing species also occurred on the Pt sites (Eq. (3)), *i.e.*, Pt was able to adsorb OH species at almost as low potentials as Ru, causing reaction also on Pt. Ru in alkaline media is not the only donor of OH_{ad} species, as is the case in acid solution:

$$Pt + OH^- \rightarrow Pt–OH_{ad} + e^- \quad (3)$$

In fact, the oxidation of CO proceeds through a quasi-bifunctional mechanism on a Pt_3Ru_2/C catalyst in acid and in alkaline solution because Pt and Ru sites adsorb CO in acid media and both metals adsorbs OH species in alkaline media.

CONCLUSIONS

The presented results can be summarized as follows:

– At a Pt_3Ru_2/C catalyst, anions (bisulfates) slightly shift the onset of the reaction towards higher potentials, thereby decreasing the reaction rate.

– A Pt_3Ru_2/C catalyst is more active in alkaline than in acid solution, since as well as Ru, Pt becomes able to adsorbed OH at low potentials, thus enhancing the reaction rate compared to acid solution.

– In acid solution, the oxidation of CO proceeds on Pt_3Ru_2/C significantly faster than on Pt/C at low potentials because Ru provides more OH_{ad} species than pure Pt.

– In alkaline solution, the oxidation of CO commences at approximately the same potential at Pt/C and at Pt_3Ru_2/C and both catalyst show similar activity at potentials up to 0.6 V.

– The oxidation of CO proceeds through a quasi-bifunctional mechanism on a Pt_3Ru_2/C catalyst in acid and in alkaline solution.

Acknowledgements. This work was financially supported by the Ministry of Science and Technological Development of the Republic of Serbia, Contract No. H-142056.

ИЗВОД

АКТИВНОСТ Pt_3Ru_2/C НАНОКАТАЛИЗАТОРА У ОКСИДАЦИЈИ CO

КСЕНИЈА Ђ. ПОПОВИЋ[1], ЈЕЛЕНА Д. ЛОВИЋ[1], АМАЛИЈА В. ТРИПКОВИЋ[1] и PIOTR K. OLSZEWSKI[2]

[1]*ИХТМ - Центар за електрохемију, Универзитет у Београду, Његошева 12, п. пр. 473, 11000 Београд и* [2]*Institute of Catalysis and Surface Chemistry, Polish Academy of Sciences, Krakow, Niezapominajek 8, 30-239, Poland*

Електрохемијска оксидација CO испитивана је на нанокатализатору Pt_3Ru_2 диспергованом на активном угљу као носачу у киселој и алкалној средини на собној температури коришћењем методе ротирајуће диск електроде (РДЕ). Катализатор је окарактерисан дифракцијом X-зрака (XRD) и добијени резултати су показали да се легура Pt_3Ru_2 састоји од две фазе: чврстог раствора Ru у Pt и од малих количина чистог Ru или чврстог раствора Pt у Ru. Електрокаталитичка активност овог катализатора за оксидацију CO је испитивана цикличном волтаметријом и показан је ефекат pH и ефекат анјона из носећег електролита. Pt_3Ru_2/C катализатор је активнији у алкалној него у киселој средини, указујући на чињеницу да у алкалији Pt може да адсорбује OH честице на исто тако ниским потенцијалима као и Ru и на тај начин убрзава реакцију оксидације CO у поређењу са киселином. Показано је да адсорпција бисулфатних анјона из носећег електролита помера почетни потенцијал реакције ка позитивнијим вредностима и смањује брзину оксидације CO. Поређењем активности Pt/C и Pt_3Ru_2/C катализатора у оксидацији CO у киселој и алкалниј средини показано је да је та разлика знатно мања у алкалној него у киселој средини.

(Примљено 23. фебруара, ревидирано 24. априла 2009)

REFERENCES

1. A. V. Tripković, K. Dj. Popović, B. N. Grgur, B. Blizanac, P. N. Ross, N. M. Marković, *Electrochim. Acta* **47** (2002) 3707
2. A. V. Tripković, S. Štrbac, K. Dj. Popović, *Electrochem. Commun.* **5** (2003) 484
3. J. D. Lović, A. V. Tripković, S. Lj. Gojković, K. Dj. Popović, D. V. Tripković, P. Olszewski, A. Kowal, *J. Electroanal. Chem.* **581** (2005) 294
4. A. V. Tripković, S. Lj. Gojković, K. Dj. Popović, J. D. Lović, A. Kowal, *Electrochim. Acta* **53** (2007) 887
5. A. V. Tripković, S. Lj. Gojković, K. Dj. Popović, J. D. Lović, *J. Serb. Chem. Soc*. **71** (2006) 1333
6. A. V. Tripković, K. Dj. Popović, J. D. Lović, *J. Serb. Chem. Soc*. **72** (2007) 1094
7. R. Parsons, T. van der Noot, *J. Electroanal. Chem.* **257** (1988) 9
8. H. A. Gasteiger, N. Marković, P. N. Ross Jr., E. J. Cairns, *J. Phys. Chem*. **98** (1994) 617
9. H. A. Gasteiger, N. Marković, P. N. Ross Jr., *J. Phys. Chem.* **99** (1995) 8290
10. M. Watanabe, S. Motoo, *J. Electroanal. Chem.* **60** (1975) 267
11. M. Watanabe, S. Motoo, *J. Electroanal. Chem.* **60** (1975) 275
12. A. Kabbibi, R. Faure, R. Durand, B. Beden, F. Hahn, J. M. Leger, C. Lamy, *J. Electroanal. Chem.* **444** (1998) 41
13. T. J. Schmidt, H. A. Gasteiger, R. J. Behm, *Electrochem. Commun.* **1** (1999) 1
14. A. Kowal, P. Olszewski, D. Tripković, R. Stevanović, *Mat. Sci. Forum* **518** (2006) 271
15. A. H. C. Sirk, J. M. Hill, S. K. Y. Kung, V. I. Birss, *J. Phys. Chem. B* **108** (2004) 689
16. G. Wu, L. Li, B.-Q. Xu, *Electrochim. Acta* **50** (2004) 1

17. S. Hadži-Jordanov, H. Angerstein-Kozlowska, M. Vuković, B. Conway, *J. Electrochem. Soc.* **125** (1978) 1471
18. T. Iwasita, *Electrochim. Acta* **47** (2002) 3663
19. K. J. J. Mayrhofer, B. B. Blizanac, M. Arenz, V. R. Stamenković, P. N. Ross, N. M. Marković, *J. Phys. Chem. B* **109** (2005) 14433
20. M. Arenz, K. J. J. Mayrhofer, V. R. Stamenković, B. B. Blizanac, T. Tomoyuki, P. N. Ross, N. M. Marković, *J. Am. Chem. Soc*. **127** (2005) 6819
21. E. A. Batista, T. Iwasita, W. Vielstich, *J. Phys. Chem. B* **108** (2004) 14216
22. Z. Jusys, J. Kaiser, R. J. Behm, *Electrochim. Acta* **47** (2002) 3693
23. D. V. Tripković, D. Strmcnik, D. van der Vilet, V. Stamenković, N. M. Marković, *Faraday Discuss.* **140** (2009) 25
24. N. P. Lebedeva, M. T. M. Koper, J. M. Feliu, R. A. van Santen, *J. Phys. Chem. B* **106** (2002) 12938
25. K. J. J. Mayrhofer, M. Arenz, B. B. Blizanac, V. R. Stamenković, P. N. Ross, N. M. Marković, *Electrochim. Acta* **50** (2005) 5144.